Two-Dimensional IR Spectroscopy

DOI: 10.1002/anie.201208625

A Hydrogen-Bond Flip-Flop through a Bjerrum-Type Defect**

*Martin Olschewski, Jörg Lindner, and Peter Vöhringer**

Linear chains of hydrogen bonds such as those formed by water wires or by arrays of hydroxy groups (···O–H···O–H···O–H···) are cooperative structural elements that play a quintessential role in defining the physico-chemical properties of homogeneous[1] and micro-heterogeneous aqueous systems,[2] of anhydrous organic,[3] inorganic,[4] and hybrid materials,[5,4b] and in channel-forming membrane proteins.[6] The nature of such extended H-bond networks is highly stochastic in space and time. Their dynamically evolving structures are characterized by hydrogen-bond disorder that is intimately linked to the appearance of structural defects similar to those originally described by Bjerrum.[7] A *D* defect arises whenever a hydrogen bond is formally occupied by two H atoms at the same time (···O–H···H–O···), while an *L* defect is formed whenever a hydrogen bond is devoid of H atoms (···H–O···O–H···). Such defects may or may not be stabilized by bridging units serving as double hydrogen donors or acceptors. H-bond disorder is a fundamental phenomenon that is responsible for the residual entropy of ice at 0 K[8] and it is connected to the maintenance of the unidirectional proton conductivity of low-dimensional H-bond networks in systems of biological and technological relevance.[9]

Dynamic H-bond disorder requires the molecular moieties of the noncovalent contacts to possess conformational flexibility and an ability to interchange their character; that is, an acceptor can become a donor and a donor can become an acceptor thereby reversing the direction of the H bond between them. In the context of extended chains and rings, H-bond disorder has been coined "flip-flop hydrogen-bonding"[10] to emphasize the coexistence of the two states with similar probability but opposite orientation, O–H···O–H⇌H–O···H–O. So far, no direct time-resolved detection of the flip-flop dynamics has been accomplished. Consequently, rates have only been indirectly estimated for very few systems[11] to be somewhere between 1/(5 ps) and 1/(50 ps).

To observe these elementary dynamics directly in the time domain, we reduced the complexity of the problem by confining the spatial extension of the H-bonded chain to a single chain element only. This archetypical structural motif is represented by the intramolecular H bond of the vicinal diol, 2,3-dimethylbutane-2,3-diol or pinacol, (Figure 1). The complexity is further reduced by dissolving the diol in a nonpolar solvent (carbon tetrachloride, room temperature) to largely suppress perturbations of the flip-flop dynamics by the molecular surroundings. Thus, our model system is of immediate relevance to nonaqueous H-bonded chains supported by organic scaffolds but the results will also impact on inorganic and biochemical systems including water wires.

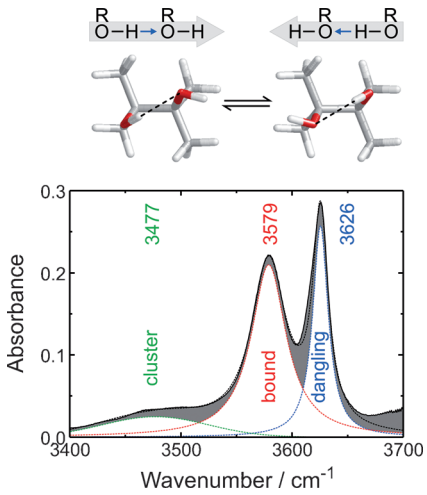

Figure 1. Top: H-bond flip-flop of the pinacol model system . Bottom: The infrared spectrum of pinacol in CCl_4 solution at 300 K can be decomposed into two bands representing the stretching vibrations of dangling (blue) and bound (red) OH oscillators. A broad and weak background absorption (green) is due to a small fraction of pinacol dimers that are irrelevant to the experiments presented here.

Infrared (IR) spectroscopy can provide valuable insight into the average structure of H-bonded systems.[12] This holds particularly true for our model system where the stretching vibrations of the two hydroxy groups engaged in the H bond can be distinguished nicely in the frequency region around 3600 cm^{-1} (see Figure 1). A rather narrow absorption band centered at 3626 cm^{-1} originates from the OH group that dangles into the nonpolar solvent and that serves as the hydrogen acceptor. A second, slightly broader absorption band centered at 3579 cm^{-1} is due to the hydrogen-donating OH group.[13] Its H-bond-induced frequency-downshift relative to the dangling hydroxy group is essentially caused by the transfer of electron density from nonbonding orbitals localized on the acceptor oxygen to antibonding orbitals of the donor.

To time-resolve the flip-flop dynamics we employed femtosecond two-dimensional IR spectroscopy (fs-2DIR), which has proven highly informative regarding the structural dynamics of H-bonded systems.[14] The basic idea of the experiment is as follows: An ultrafast IR pump-pulse photo-

[*] M. Olschewski, Dr. J. Lindner, Prof. Dr. P. Vöhringer
Institut für Physikalische und Theoretische Chemie
Rheinische Friedrich-Wilhelms-Universität
Wegelerstrasse 12, 53115 Bonn (Germany)
E-mail: p.voehringer@uni-bonn.de
Homepage: http://www.chemie.uni-bonn.de/pctc/voehringer

[**] This work was supported by the Deutsche Forschungsgemeinschaft through SFB 624 and SFB 813.

Supporting information for this article is available on the WWW under http://dx.doi.org/10.1002/anie.201208625.

excites the dangling (or alternatively, the bound) OH oscillators. This depopulates the vibrational ground state of the dangling (bound) OH, which can be detected as an increased transmission/stimulated emission of a variably delayed broadband probe-pulse at the pump-pulse frequency. During the pump-probe time delay, a fraction of the dangling OH groups may transform into bound OH groups and vice versa. If the lifetimes of the vibrational excited states are sufficiently long, the oscillators retain their vibrational excitation during the H-bond reversal. Thus, an initially photo-excited dangling (bound) OH group may become visible through a stimulated emission of the broadband probe-pulse at the resonance of the bound (dangling) OH. In other words, the H-bond flip-flop may cause a chemical exchange between the stretching resonances of the dangling and bound OH groups.

Figure 2 displays a series of 2DIR spectra of the diol for various pump-probe delays. At a delay of 700 fs, the spectrum features along the diagonal axis ($\nu_{probe} = \nu_{pump}$) the expected

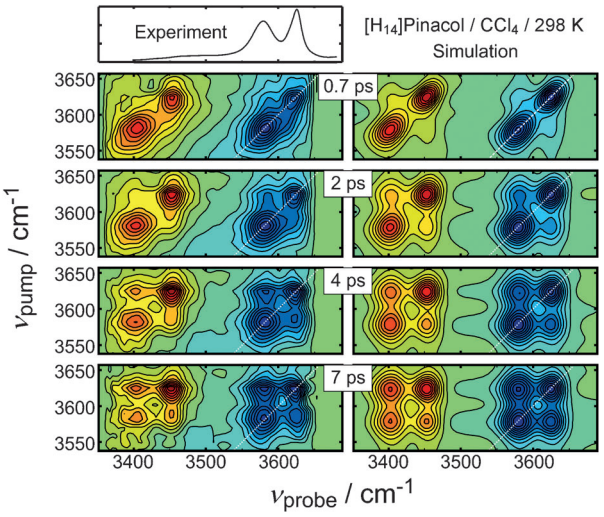

Figure 2. Series of experimental 2DIR spectra of pinacol (left column, in CCl_4 solution, 300 K) at various time delays and complementary simulations (right columm, see text for details). The linear FTIR spectrum is shown in the top left panel. The diagonal axis (where $\nu_{probe} = \nu_{pump}$) is indicated by the dashed white line. At 700 fs, only the diagonal signal pairs of bleach/emission (cyan-to-blue contours) and transient absorption (yellow-to-red) are visible. At later delays, the appearance of additional cross peaks indicates a dynamic exchange between the two types of OH oscillators due to H-bond flip-flop.

increased transmission/stimulated emission at the two fundamental $v = 0 \rightarrow 1$ transitions. In addition, since the vibrational excited states were populated by the pump-pulse, two induced absorptions of the $v = 1 \rightarrow 2$ transitions appear that are shifted to lower probe frequencies (i.e. $\nu_{probe} < \nu_{pump}$) due to the diagonal anharmonicity of the two OH stretching vibrations. As the time delay gradually increases, highly characteristic off-diagonal peaks appear. Such cross-peaks can be observed in the spectral regions of both the $v = 0 \rightarrow 1$ and the $v = 1 \rightarrow 2$ transitions. A movie displaying a full time-series of fs-2DIR spectra from 700 fs up to 10 ps is given in the Supporting Information. The delayed appearance of cross-peaks demonstrates that vibrational excitation is indeed transferred between dangling and bound hydroxy oscillators of the model system. Complementary experiments have also been carried out on isotopically labeled pinacols as well as on mixtures of isotopomers to unambiguously establish that the cross-peak appearance is indeed related to the H-bond reversal and not to an equilibration of the vibrational populations in the two OH stretching excited states by virtue of vibrational energy relaxation or resonant energy transfer (see the Supporting Information).

For a quantification of the H-bond flip-flop dynamics, the 2DIR data were simulated within the framework of nonlinear response functions[15] using two interconverting species, namely pinacol configurations with a left-to-right and a right-to-left oriented hydrogen bond. The simulations are also shown in Figure 2 and the required fitting parameters are compiled in the Supporting Information. As can be seen, the agreement between experiment and simulation is excellent. The simulations return an exchange rate of 1/(2.1 ps). Notice that for symmetry reasons, the forward and backward rates for the H-bond flip-flop are identical, that is, 1/(4.2 ps). Furthermore, for the deuterated pinacol, $(CH_3)_2C(OD)$-$C(OD)(CH_3)_2$, an exchange rate of 1/(6.0 ps) is obtained, thereby revealing a pronounced kinetic isotope effect.

To understand the H-bond flip-flop mechanism at the molecular level, density functional theory (DFT, B3LYP/6-311++G**) calculations were conducted. Disregarding the internal methyl rotors, the molecular structure of the diol can be specified by the two CC-OH dihedral angles (θ and Φ) and the OC-CO torsional angle, γ (Figure 3a). The optimized structure (labeled structure **2**) corresponds to the set of dihedrals angles, $\Phi = 162.3°$, $\theta = 48.4°$, and $\gamma = -54.7°$ with an O···O distance of 2.67 Å and an H-bond length of 2.15 Å. A

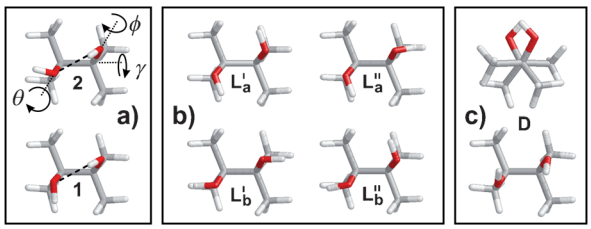

Figure 3. a) DFT-optimized structures **1** and **2** of pinacol and the torsional angles relevant to H-bond flip-flop. b) Bjerrum-type *L* defects. c) Bjerrum-type *D* defect viewed from two different perspectives.

second deep minimum (structure **1**) exists at $\Phi = 80.1°$, $\theta = 43.0°$, $\gamma = -50.6°$, and similar H-bond geometry, which lies roughly 50 cm^{-1} above **2**. Basically, these two geometries differ only in the lone electron pair of the acceptor oxygen that is responsible for H bonding.

Subsequently, a potential energy surface (PES), $V(\theta, \Phi)$, relevant to the H-bond flip-flop motion was constructed by scanning along the angles, θ and Φ, while relaxing all other internal coordinates including γ. As shown in Figure 4a, this PES is a highly complex, corrugated landscape with many local minima and maxima resulting essentially from the four

lone pairs at the two sp^3-hybridized oxygen atoms that can engage in H bonding. Four energetically high-lying minima can be identified as Bjerrum-type *L* defects (cf. Figure 3b), which are either symmetric ($\theta = \Phi$, $\mathbf{L'}_a$ and $\mathbf{L'}_b$) or asymmetric ($\theta \neq \Phi$, $\mathbf{L''}_a$ and $\mathbf{L''}_b$) with respect to the CC-OH dihedral angles. Furthermore, a characteristic *D* defect is also identified as a stationary point on the PES. As displayed in Figure 3c, it is symmetric with regard to the CC-OH torsion angles ($\theta = \Phi = 79.4°$, $\gamma = -54.6°$) and features an O···O distance of 2.72 Å. Its H atoms are separated by only 2.28 Å and thus, by less than the sum of their van der Waals radii (2.4 Å).[16] Nevertheless, this Bjerrum-type *D* defect lies only 240 cm^{-1} above the global minimum structure, **2**, and must therefore be significantly populated at room temperature.

Most intriguingly, the PES exhibits a deep valley interconnecting energy minima associated with a left-to-right oriented hydrogen bond, that is, structures **1** and **2**, with those that are linked with a right-to-left oriented hydrogen bond, structures **3** and **4**. The valley runs right through the *D* defect and encompasses energy barriers whose heights are comparable to the thermal excitations. The minimum-energy path (MEP), where $dV/d\Phi = 0$ for fixed θ within the valley, constitutes the reaction coordinate for H-bond flip-flop and is included in Figure 4a as the dashed curve.

The sequence of molecular structures adopted along this extraordinary coordinate is presented in Figure 4b and in more detail as an animation in the Supporting Information. A cut through the PES along the MEP is displayed in Figure 4c together with the Boltzmann density at room temperature. The latter is fully smeared out across all wells and barriers, thereby confirming that the system is fully fluxional and that the H bond can spontaneously reverse its direction. Starting with the left-to-right oriented H-bond configuration of **1** the system can evolve by switching its acceptor's lone pair to adopt the global minimum structure, **2**. The lone-pair switching involves a clockwise rotation of the dangling OH with almost negligible reorientation of the bound OH and requires the crossing of a barrier with a height of about 280 cm^{-1}. The system can carry on rotating its dangling OH in a clockwise direction; however, the continued motion is now strongly coupled to a counterclockwise reorientation of the bound OH. This synchronous disrotatory torsion of the two hydroxy groups leads over a barrier of 248 cm^{-1} towards the shallow minimum of the *D* defect. The latter appears weakly bound by about 10 cm^{-1} and a continuation of the concerted motion along the two OH dihedral angles leads to structure **3**, the energetically degenerate right-to-left oriented counterpart of **2**. Finally, the sequence can be completed by another lone-pair switching event, which requires the system to surmount a barrier of 330 cm^{-1} and to arrive at the original, but now right-to-left oriented structure **4**.

An instantaneous vibrational analysis along the MEP (see Figure 4d) demonstrates that the H-bond flip-flop couples to the two OH stretches; that is, their frequencies strongly

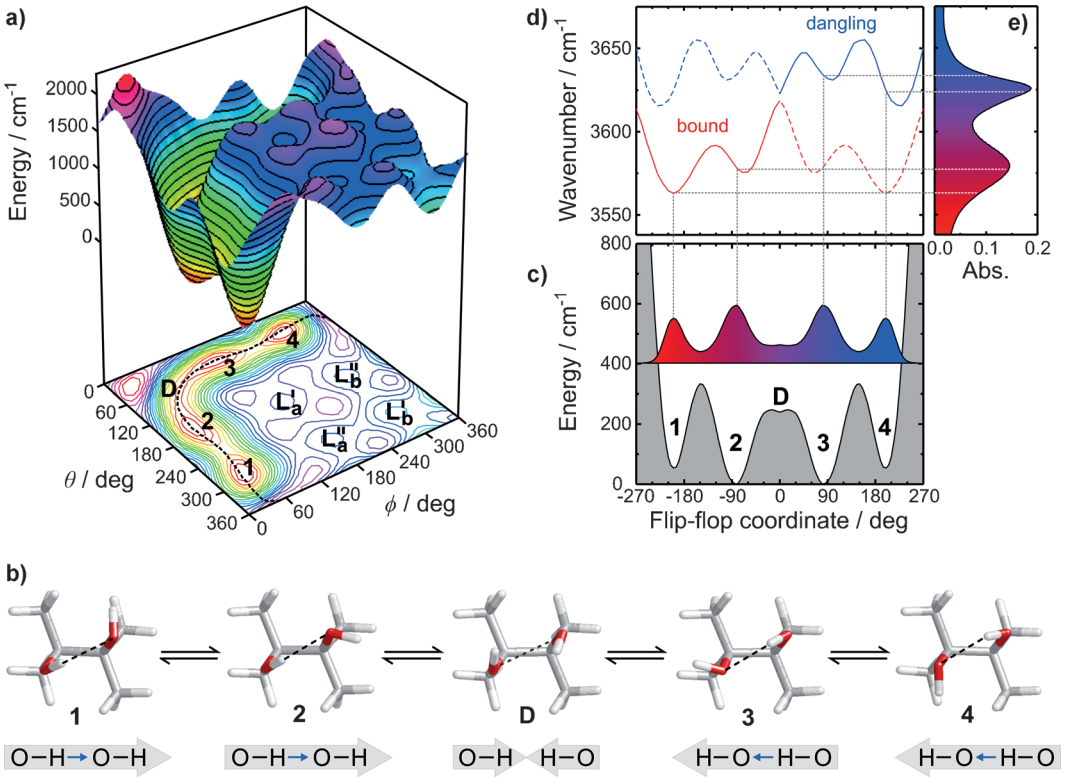

Figure 4. a) PES relevant to H-bond flip-flop. The MEP is indicated by the dashed curve in the contour representation at the bottom. b) Sequence of molecular structures during H-bond flip-flop. c) One-dimensional cut through the PES (gray) and Boltzmann density (red–blue) at room temperature. d,e) Instantaneous OH-stretching frequencies along the MEP and FTIR spectrum of pinacol (red–blue).

depend on the relative alignment of the two hydroxyl groups. The OH vibrations of structures **1** through **4** are negligibly coupled and are best described as local modes, while those of the *D* defect become symmetry-degenerate and split into symmetric and antisymmetric combinations. Moving through this unique structure swaps the mode assignment: what has initially been a dangling OH now becomes a bound OH and vice versa. Figure 4d uniquely demonstrates that thermally induced structural fluctuations along the flip-flop coordinate results in fluctuations of the OH stretching frequencies. They are responsible for a broadening of the two OH stretching bands and most importantly, for the dynamic exchange between dangling and bound hydroxy resonances as seen in Figure 2 as cross-peaks appearing with increasing delay.

Lastly, we crudely estimate the rate of the H-bond flip-flop from the unidirectional lifetime of a *D* defect decaying into either a left-to-right (**D**→**2**) or to a right-to-left (**D**→**3**) oriented H bond. The attempt frequency for this reaction corresponds to the frequency of the bound motion of the *D* defect along the reaction coordinate, that is, along the synchronous disrotatory CC-OH torsions. The *D* defect features indeed such a normal mode with a harmonic frequency of $\nu_0 = 46\ cm^{-1}$. The rate of escape[17] from the *D*-defect well is estimated by the classical transition state theory expression $k_{D\rightarrow 2} = \nu_0 \exp(-\Delta E_{D\rightarrow 2}/k_B T)$, where $\Delta E_{D\rightarrow 2} = 10\ cm^{-1}$ is the barrier height for the **D**→**2** decay. The rate for the reverse reaction, that is, the formation of **D** from a left-to-right oriented hydrogen bond is given by detailed balance, that is, $k_{2\rightarrow D} = k_{D\rightarrow 2} \exp(-\Delta E_{2\rightarrow D}/k_B T)$. With $\Delta E_{2\rightarrow D} = 248\ cm^{-1}$ from the DFT calculations, we arrive at a value for $k_{2\rightarrow D}$ of 1/(2.5 ps). In terms of phenomenological kinetics, the unidirectional H-bond flip-flop can be decomposed into two consecutive unimolecular processes, **2**→**D**→**3**: a slower formation of the *D* defect from the left-to-right oriented structure **2** with a rate of $k_{2\rightarrow D} = 1/(2.5\ ps)$ and a subsequent faster decay of the *D* defect into the right-to-left oriented structure **3** with a rate of $k_{D\rightarrow 3} = k_{D\rightarrow 2} = 1/(0.76\ ps)$. Note, at thermal equilibrium the reverse process, **3**→**D**→**2**, occurs at exactly the same consecutive rates.

A few issues are worth emphasizing at this stage. In simulating the 2DIR spectra we represented the flip-flop dynamics by a two-state model while we have predicted the exchange rates from a consecutive reaction mechanism involving the *D* defect as an intermediate. Since the 2DIR data do not indicate any pump-induced perturbation of the flip-flop equilibrium, the exchange rate retrieved from modeling the 2DIR data should be compared with the slower rate-limiting step of *D*-defect formation. Therefore, the experimental unidirectional exchange rate of 1/(4.2 ps) is in reasonable agreement with the above crude estimate of 1/(2.5 ps) based on transition state theory. More importantly, a classical rate was calculated despite the fact that the shallow *D*-defect well does not support a quantum-mechanical vibrational zero-point level. Therefore, the *D* defect cannot be regarded as a stable configuration and a decomposition of the dynamics into two consecutive unimolecular barrier crossings formally fails. In the future, we will address this intriguing issue through ab initio molecular dynamics simulations of the H-bond flip-flop phenomenon.

In conclusion, using fs-2DIR exchange spectroscopy we have observed for the first time the elementary dynamics of a hydrogen-bond flip-flop. This fundamentally important process was studied using the intramolecular H bond of a vicinal diol as a model system for the archetypical structural unit of extended chains of hydroxy residues. The H-bond reversal is thermally activated; it occurs on a timescale of roughly 2 ps, and it is facilitated by a molecular mechanism that involves two synchronous disrotatory CC-OH single-bond torsional isomerizations. Motion along the reaction coordinate guides the system through a Bjerrum-type *D* defect whose hydrogen bond is formally occupied by two hydrogen atoms at the same time.

Received: October 26, 2012
Revised: December 26, 2012

Keywords: Bjerrum defects · hydrogen bonds · infrared spectroscopy · proton transfer · two-dimensional IR spectroscopy

[1] O. F. Mohammed, D. Pines, J. Dreyer, E. Pines, E. T. J. Nibbering, *Science* **2005**, *310*, 83–86.
[2] K. D. Kreuer, S. J. Paddison, E. Spohr, M. Schuster, *Chem. Rev.* **2004**, *104*, 4637–4678.
[3] L. Jimenez-Garcia, A. Kaltbeitzel, W. Pisula, J. S. Gutmann, M. Klapper, K. Mullen, *Angew. Chem.* **2009**, *121*, 10135–10138; *Angew. Chem. Int. Ed.* **2009**, *48*, 9951–9953.
[4] a) S. M. Haile, D. A. Boysen, C. R. I. Chisholm, R. B. Merle, *Nature* **2001**, *410*, 910–913; b) D. Umeyama, S. Horike, M. Inukai, T. Itakura, S. Kitagawa, *J. Am. Chem. Soc.* **2012**, *134*, 12780–12785.
[5] a) H. Steininger, M. Schuster, K. D. Kreuer, A. Kaltbeitzel, B. Bingol, W. H. Meyer, S. Schauff, G. Brunklaus, J. Maier, H. W. Spiess, *Phys. Chem. Chem. Phys.* **2007**, *9*, 1764–1773; b) J. A. Hurd, R. Vaidhyanathan, V. Thangadurai, C. I. Ratcliffe, I. L. Moudrakovski, G. K. H. Shimizu, *Nat. Chem.* **2009**, *1*, 705–710.
[6] F. Garczarek, K. Gerwert, *Nature* **2006**, *439*, 109–112.
[7] N. Bjerrum, *Science* **1952**, *115*, 385–390.
[8] S. J. Singer, C. Knight, *Adv. Chem. Phys.* **2012**, *147*, 1–74.
[9] R. Pomès, B. Roux, *Biophys. J.* **2002**, *82*, 2304–2316.
[10] W. Saenger, C. Betzel, B. Hingerty, G. M. Brown, *Nature* **1982**, *296*, 581–583.
[11] a) T. Steiner, W. Saenger, R. E. Lechner, *Mol. Phys.* **1991**, *72*, 1211–1232; b) M. G. Usha, R. J. Wittebort, *J. Am. Chem. Soc.* **1992**, *114*, 1541–1548.
[12] A. Kandratsenka, D. Schwarzer, P. Vöhringer, *J. Chem. Phys.* **2008**, *128*, 244510–244516.
[13] A. J. Lock, J. J. Gilijamse, S. Woutersen, H. J. Bakker, *J. Chem. Phys.* **2004**, *120*, 2351–2358.
[14] J. R. Zheng, K. Kwak, J. Asbury, X. Chen, I. R. Piletic, M. D. Fayer, *Science* **2005**, *309*, 1338–1343.
[15] K. Kwak, J. R. Zheng, H. Cang, M. D. Fayer, *J. Phys. Chem. B* **2006**, *110*, 19998–20013.
[16] A. Bondi, *J. Phys. Chem.* **1964**, *68*, 441–451.
[17] A. Nitzan, *Chemical Dynamics in Condensed Phases*, Oxford University Press, New York, **2006**.

